Published in final edited form as:
Cell. 2015 February 26; 160(5): 1013–1026. doi:10.1016/j.cell.2015.01.038.

A platform for rapid exploration of aging and diseases in a naturally short-lived vertebrate

Itamar Harel[1], **Bérénice A. Benayoun**[1], **Ben Machado**[1], **Param Priya Singh**[1], **Chi-Kuo Hu**[1], **Matthew F. Pech**[2,3], **Dario R. Valenzano**[1,4], **Elisa Zhang**[1], **Sabrina C. Sharp**[1], **Steven E. Artandi**[2,3,5], and **Anne Brunet**[1,5,6]

[1]Department of Genetics, Stanford University, Stanford, CA 94305, USA

[2]Department of Medicine, Stanford University School of Medicine, Stanford, CA 94305, USA

[3]Biochemistry Department, Stanford University School of Medicine, Stanford, CA 94305, USA

[5]Glenn Laboratories for the Biology of Aging at Stanford, Stanford, CA 94305, USA

Summary

Aging is a complex process that affects multiple organs. Modeling aging and age-related diseases in the lab is challenging because classical vertebrate models have relatively long lifespans. Here we develop the first platform for rapid exploration of age-dependent traits and diseases in vertebrates, using the naturally short-lived African turquoise killifish. We provide an integrative genomic and genome-editing toolkit in this organism using our *de novo*-assembled genome and the CRISPR/Cas9 technology. We mutate many genes encompassing the hallmarks of aging, and for a subset, we produce stable lines within 2–3 months. As a proof-of-principle, we show that fish deficient for the protein subunit of telomerase exhibit the fastest onset of telomere-related pathologies among vertebrates. We further demonstrate the feasibility of creating specific genetic variants. This genome-to-phenotype platform represents a unique resource for studying vertebrate aging and disease in a high throughput manner and for investigating candidates arising from human genome-wide studies.

[6]Corresponding author: abrunet1@stanford.edu.
[4]Present address: Max Planck Institute for Biology of Ageing, Cologne 50931, Germany

Author Contributions

I.H. and A.B. designed the study and wrote the manuscript. I.H. performed experiments with help from B.M. B.A.B. generated gene models with help from P.P.S. and E.Z. B.A.B also analyzed all datasets generated by D.R.V. (genomic), C.K.H. (transcriptomic), and I.H. (epigenomic). P.P.S. performed the protein domain conservation analysis. M.F.P. and S.E.A. helped I.H. with the telomerase related assays. S.C.F. helped I.H. with injections. All authors commented on the manuscript.

Accession Numbers

Sequencing and genome data have been deposited to the Genbank (JNBZ00000000). RNA sequencing (SRP041421) and H3K4me3 ChIP-seq (SRP045718) data were submitted to SRA (sequence read archive).

Introduction

Aging is the number one risk factor for many human pathologies, including diabetes, cancer, cardiovascular, and neurodegenerative diseases (Niccoli and Partridge, 2012). Thus, delaying aging could help postpone the onset of these devastating ailments and increase healthspan. Because aging affects multiple organs and systems in humans (Lopez-Otin et al., 2013), it is one of the most challenging processes to model in the lab. So far, the study of aging has been dominated by non-vertebrate short-lived model organisms, such as yeast (*C. cerevisiae*), worm (*C. elegans*) and fly (*D. melanogaster*), which has allowed the identification of remarkably conserved aging-related pathways, such as the TOR and Insulin/IGF pathways (Kenyon, 2010). However, some important aspects of human aging and disease phenotypes cannot be faithfully recapitulated in invertebrate models, as they lack specific organs and systems (e.g. blood, bones, and an adaptive immune system) that are crucial components of human aging and age-related pathologies. Vertebrate model systems, namely the mouse (*M. musculus*) and zebrafish (*D. rerio*), have also been exploited to probe genes involved in aging and age-related diseases. However, experimental studies have been hampered by the relatively long lifespan of mice and zebrafish (maximal lifespan of 3–4 and 5 years, respectively (Tacutu et al., 2013)) and high costs of maintenance, especially for mice. Mouse models with accelerated onset of age-associated disease (e.g. neurodegeneration) can partially address this issue (Trancikova et al., 2010), but these models uncouple the disease phenotype from its main risk factor – aging – and they remain expensive to use. Thus, a new vertebrate model is needed to better understand the principles of vertebrate aging and to study age-related diseases in the context of aging.

The African turquoise killifish *Nothobranchius furzeri* is a naturally short-lived vertebrate that lives in ephemeral water ponds in Zimbabwe and Mozambique (Figure 1A), where water is only present during a brief rainy season. This fish species has likely evolved a compressed life-cycle (as short as 40 days from egg to egg-laying adult) to adapt to its transient habitat. The turquoise killifish is currently the shortest-lived vertebrate that can be bred in captivity (Genade et al., 2005; Valenzano et al., 2006), with a lifespan of 4–6 months in optimal laboratory conditions (6 to 10 times shorter than the lifespan of mice and zebrafish, respectively). Importantly, despite its short lifespan, this fish recapitulates typical age-dependent phenotypes and pathologies such as decline in fertility, sarcopenia, cognitive decline, and cancerous lesions (Di Cicco et al., 2011; Genade et al., 2005; Valenzano et al., 2006). It also displays a conserved response to environmental stimuli known to affect the aging rate in other species, such as dietary restriction (Terzibasi et al., 2009). These characteristics make this fish an attractive model organism to study vertebrate aging, physiology and age-dependent diseases throughout organismal lifespan (Di Cicco et al., 2011). Furthermore, the turquoise killifish telomeres are similar in length to those of humans (6–8kb) (Hartmann et al., 2009), unlike laboratory mouse telomeres which are very long (50–150 kb) (Lee et al., 1998). Thus, findings from aging studies in the turquoise killifish should be relevant for vertebrate aging, including humans. The rapid time scale of aging in this species should not only facilitate the causative identification of factors regulating vertebrate lifespan, but also allow longitudinal studies.

The turquoise killifish has additional advantages as a model system. Contrary to many other fish, including zebrafish, the turquoise killifish has a XY-based sexual determination (Valenzano et al., 2009). Furthermore, there exists a highly inbred strain of the turquoise killifish (the GRZ strain, used in this study), as well as a number of wild-derived strains (Terzibasi et al., 2008). The availability of multiple strains provides an important advantage for genetic studies and for mapping traits that are different between strains (e.g. color, maximal lifespan) (Kirschner et al., 2012; Valenzano et al., 2009). Collectively, these characteristics of the turquoise killifish – coupled with the ease of rapidly generating many offspring and low maintenance costs – make this fish a promising vertebrate model, uniquely fit to address aging and age-related diseases (Genade et al., 2005; Valenzano et al., 2006).

For the African turquoise killifish to become a widely used vertebrate model compatible with high throughput approaches, key tools need to be created. While preliminary genetic tools have been developed in the turquoise killifish, including genetic linkage maps (Kirschner et al., 2012; Reichwald et al., 2009; Valenzano et al., 2009), and Tol2-based transgenesis (Hartmann and Englert, 2012; Valenzano et al., 2011), the lack of a sequenced genome and ability to manipulate endogenous genes has drastically limited the use of this organism. The RNA-guided CRISPR (clustered regularly interspaced short palindrome repeats) associated Cas9 nuclease (Jinek et al., 2012) has recently emerged as an effective approach for introducing targeted mutations in a variety of model organisms, such as yeast, worms, flies, zebrafish, and mice, as well as several non-model organisms (for a detailed list see (Hsu et al., 2014)). However, genome-editing approaches have never been reported in the African turquoise killifish, probably because of the lack of a sequenced genome.

Here we create the first platform for the rapid exploration of aging and aging-related diseases in vertebrates by developing new genomic and genome-editing tools in a promising vertebrate model, the naturally short-lived African turquoise killifish. As a proof of principle for the versatility of this platform, we generate a suite of mutated alleles for 13 genes encompassing the hallmarks of aging and report 6 stable lines to date. We characterize a loss-of-function mutation in the gene encoding the protein component of telomerase, and show that telomerase-deficient turquoise killifish recapitulate characteristics of human pathologies. This platform should allow high throughput studies on aging and longevity in vertebrates, as well as longitudinal modeling of human diseases. Our platform should also enable systematic examination of unexplored candidates identified in human genomic studies.

Results

A platform for the study of ‘hallmarks of aging’ genes in vertebrates

We sought to create a versatile platform to rapidly model human aging and diseases in the short-lived turquoise killifish (Figure 1A). A recent review has categorized 9 ‘hallmarks of aging’ (Lopez-Otin et al., 2013), including telomere attrition, deregulated nutrient sensing, and stem cell exhaustion (Figure 1B). We selected 13 genes encompassing those hallmarks (e.g. the protein subunit of telomerase [TERT], insulin-like growth factor 1 receptor

[IGF1R], S6 kinase [RPS6KB1]) with the overall goal of generating mutant alleles for each of them (Figure 1B).

Because the turquoise killifish is an emerging model, the first step was to identify genes in this organism. To this end, we generated a wide range of genomic datasets and designed a tailored genomic pipeline. We built gene models, using our recently assembled turquoise killifish genome (Figure 1C). We verified the accuracy of gene models and analyzed mRNA expression pattern using our RNA-seq datasets from four tissues (Figure 1C). We generated an H3K4me3 ChIP-seq dataset to define transcriptional start sites (TSSs) and further support annotations, especially for non-coding RNAs (Rinn and Chang, 2012) (Figure 1C). Additional support for protein-coding gene annotation was obtained using protein homology (Figure 1C). Finally, we designed guide RNA (gRNA) targets for CRISPR/Cas9 genome-editing (Figure 1C and Table S1). The genome of the turquoise killifish and the RNA-seq and H3K4me3 ChIP-seq datasets are provided as resources (accession numbers: JNBZ00000000, SRP041421, and SRP045718, respectively). The full description and analysis of the genome will be reported elsewhere (D.R.V., B.A.B., P.P.S., and A.B., unpublished data). The gene models and gRNA design are made available via the CHOPCHOP platform (https://chopchop.rc.fas.harvard.edu/) (Montague et al., 2014). Together, these datasets provide an integrative resource for the scientific community, not only to target specific genes in the turquoise killifish, but also for comparative genomics and evolutionary studies of aging and longevity.

We then designed a CRISPR/Cas9 genome-editing strategy in the turquoise killifish. Based on our tailored genomic pipeline, we generated two to five independent gRNA sequences for each gene (Table S1). We then microinjected a mixture of Cas9 mRNA and gRNAs into fertilized turquoise killifish eggs at the single-cell stage (Hwang et al., 2013; Jao et al., 2013) (Figure 1D). Cas9 is known to introduce double-strand breaks that are repaired by non-homologous end joining (NHEJ), resulting in genome editing (small deletions or insertions, also known as indels) (Hsu et al., 2014). Successful editing was assessed in a subset of eggs by cloning and sequencing of the targeted region 72h after injection (Figure 1D, Step 1). The gRNAs that resulted in successful editing were then used to generate F0 chimeras that were crossed with wild-type fish to generate F1 embryos (Figure 1D, Step 2). Successful germline transmission was assessed on pooled F1 embryos, usually 45–60 days after initial injection (Figure 1D, Step 3). F1 embryos from successful F0 chimeras (founders) were raised to adulthood, and fish with desired alleles maintained as stable lines and further backcrossed to minimize potential off-target editing by Cas9 (Figure 1D, Step 4). We will first describe our results with *TERT* as a paradigm for modeling telomere attrition, and then present the general toolbox of 13 mutant alleles in genes involved in the hallmarks of aging.

Modeling telomere attrition

Telomerase, which comprises the protein component TERT and the RNA component *TERC*, elongates telomeres after replication, thereby maintaining telomere length (Figure 2A). Telomeres shorten during vertebrate aging, including in the turquoise killifish (Artandi and DePinho, 2010; Hartmann et al., 2009), and are considered to be a good biomarker of

biological age (Boonekamp et al., 2013). In humans, mutations in *TERT* or other genes in the telomere-protecting complex result in a spectrum of diseases characterized by tissue homeostasis failure, such as dyskeratosis congenita (Armanios, 2009). Dyskeratosis congenita patients exhibit multiple symptoms resembling aspects of premature aging, including bone marrow failure and pulmonary fibrosis (Armanios, 2009), reduced fertility (Bessler et al., 2010), and several types of cancers (Alter et al., 2009). Because of their long telomeres, TERT-deficient laboratory mice have to be bred for 4–6 generations for disease phenotypes to manifest (Lee et al., 1998), and are therefore not ideal to model human TERT deficiency or telomere attrition during aging.

We first asked if telomerase components are conserved in the turquoise killifish (Figure 2A). The *TERT* gene model (Figure 2A) allowed us to predict a putative TERT protein sequence in the turquoise killifish. The predicted TERT protein was conserved, particularly in the RNA binding and the reverse transcriptase (RT) catalytic domains (Figure 2B). The sequence divergence between *TERT* from the turquoise killifish and other species precisely matched the evolutionary tree (Figure 2C), confirming that the predicted TERT protein indeed corresponds to turquoise killifish TERT. Interestingly, our RNA-seq data revealed that *TERT* mRNA expression was enriched in the testis relative to other tissues in the turquoise killifish, similar to what is observed in humans (Bessler et al., 2010) (Figure 2D). *TERC*, the RNA component of telomerase, as well as other genes encoding proteins associated with telomerase (e.g. *DYSKERIN*) or involved in the protection of telomeres (e.g. *TERF2* from the Shelterin complex) were also present and expressed in the turquoise killifish (Figures 2A and S1). Thus, telomerase components are well conserved between human and the turquoise killifish.

To edit the *TERT* gene in the turquoise killifish, we designed two guide-RNAs (gRNAs) with a targeting region within the *TERT* exon 2 – a long exon located upstream to both catalytic domains of TERT (the RNA binding and the RT domains) (Figure 2F, upper panel). One of the two guide-RNAs led to the generation of a range of deletions in the targeted region of the *TERT* gene (from 3bp to 15bp), with a frequency of 10% (Figure 2E). By raising the injected embryos to sexual maturity (~40 days), we obtained four F0 chimeras. Crossing each of these four chimeras with wild-type fish allowed us to generate stable lines with two different types of deletion in *TERT*: 3bp (Δ3) and 8bp (Δ8) (Figure 2E). The Δ*8 TERT* allele was successfully transcribed, as assessed by PCR amplification and sequencing of cDNA from heterozygous fish (Figure 2F, bottom panel). The Δ *8 TERT* allele is predicted to give rise to a premature stop codon in the TERT protein, N-terminal to the catalytic domains (Figure 2F). These results demonstrate the feasibility for rapid genome manipulation in the turquoise killifish, with a total time from injection to stable line of about 2months.

A TERT-deficient line in the turquoise killifish exhibit loss of telomerase function and are outwardly normal

We characterized the fish harboring the Δ*8 TERT* allele, which is predicted to result in a TERT protein without catalytic activity. To reduce the frequency of potential off-target mutations, we backcrossed $TERT^{\Delta 8/+}$ fish for 3 generations. We then crossed these

heterozygous fish with each other to generate *TERT*$^{\Delta 8/\Delta 8}$ homozygous individuals (Generation 1 of homozygous individuals, G1) (Figure 3A). The ratio of adult G1 *TERT*$^{\Delta 8/\Delta 8}$ mutants followed the expected Mendelian ratio (P = 0.8809, χ^2 test) (Figure 3A), indicating no embryonic or juvenile (fry) lethality. Furthermore, G1 *TERT*$^{\Delta 8/\Delta 8}$ embryos and adult fish were outwardly normal (Figures 3B and S2A). We asked whether the *TERT*$^{\Delta 8/\Delta 8}$ allele was a true loss-of-function using the Telomere Repeat Amplification Protocol (TRAP) (Figure 3C). In this assay, tissue extracts are incubated with a radiolabeled oligonucleotide template, followed by PCR amplification of elongated products and autoradiography (Figure 3C). This protocol allowed us to assess telomerase enzymatic activity in liver extracts from *TERT*$^{+/+}$ (wild-type) and *TERT*$^{\Delta 8/\Delta 8}$homozygous siblings (Figure 3D). While liver extracts from wild-type fish showed robust telomerase activity, we failed to detect any telomerase activity in extracts from *TERT*$^{\Delta 8/\Delta 8}$ fish (Figure 3D). Thus, the Δ*8* allele of *TERT*, which is predicted to generate a truncated TERT protein, leads to a complete loss of telomerase activity and outwardly normal individuals.

TERT-deficient fish have age-dependent defects in the germline

Most human patients with haploinsufficiency for telomerase develop normally but exhibit a broad spectrum of tissue homeostasis failure (Armanios, 2009), especially in highly proliferative tissues such as blood, skin, intestine, and male germline (Bessler et al., 2010). TERT is highly expressed in the germline (Bessler et al., 2010) and is considered to be particularly important for maintaining the 'immortality' of the germline (Zucchero and Ahmed, 2006). We first tested the fertility of young (2 month old) G1 *TERT*$^{\Delta 8/\Delta 8}$ males compared to control (heterozygous) siblings by crossing them to young wild-type females (Figure 3E). While control heterozygous male fish were able to fertilize the majority of eggs (81%), G1 *TERT*$^{\Delta 8/\Delta 8}$ males only fertilized 9% of eggs, indicating a dramatic reduction in fertility (Figure 3F, $p<0.01$, Wilcoxon signed-rank test). Older G1 *TERT*$^{\Delta 8/\Delta 8}$ males (4 month old) showed a further decline in fertility (Figure 3F, $p<0.05$, Wilcoxon signed-rank test, comparison between age groups). Consistently, the testes of older G1 *TERT*$^{\Delta 8/\Delta 8}$ males were atrophied and had an almost complete loss of germ cells compared to age-matched wild-type controls (Figure 3G, black arrowheads). Germ cells were present in younger G1 *TERT*$^{\Delta 8/\Delta 8}$ males (Figure 3G, inserts), suggesting an age-dependent defect of the germline. Similarly, G1 *TERT*$^{\Delta 8/\Delta 8}$ females also had atrophied ovaries (Figure S2B) and laid fewer eggs than wild-type controls (average of 7±4, and 74±25 eggs respectively, Figure S2B). Thus, G1 *TERT*$^{\Delta 8/\Delta 8}$fish show premature defects in their germline, resulting in infertility.

G1 *TERT*$^{\Delta 8/\Delta 8}$ fish also displayed defects in other highly proliferative tissues, including blood (overall decrease in tested blood cell types, Figure S2C) and intestine (villi atrophy in some gut regions, Figure S2C). Furthermore, as previously reported in mouse models for TERT (Artandi and DePinho, 2010; Hao et al., 2005), TERT-deficient fish exhibited epithelial adenomatous changes (decreased polarity and increased nuclear/cytoplasmic ratio) (Figure S2D), which could represent a first step toward intestinal cancers such as those found in dyskeratosis congenita patients (Alter et al., 2009). In contrast, these older G1 *TERT*$^{\Delta 8/\Delta 8}$ fish did not exhibit significant defects in low-proliferative tissues such as heart, muscle, liver, and kidney (Figure S2E). As the *TERT*$^{\Delta 8/\Delta 8}$ turquoise killifish model exhibits phenotypes in the first generation (as opposed to several generations in laboratory mice (Lee

et al., 1998)) and within 2 months (as opposed to 6–8 months in zebrafish (Anchelin et al., 2013; Henriques et al., 2013)), it is currently the fastest system to study telomere attrition pathologies in vertebrates.

TERT-deficient fish exhibit signs of 'genetic anticipation'

To further explore the effect of TERT deficiency on the germline, we tested whether the offspring of TERT-deficient fish exhibit signs of 'genetic anticipation'. Genetic anticipation is a phenomenon in which symptoms of a genetic disorder are increased in severity or become apparent at an earlier age in the next generation, mostly due to cumulative damage in the germline. Dyskeratosis congenita patients show genetic anticipation: offspring of affected individuals often exhibit earlier onset and more severe symptoms as well as shorter telomeres (Savage and Alter, 2009). To test if $TERT^{\Delta 8/\Delta 8}$ fish also showed signs of genetic anticipation, we crossed the G1 $TERT^{\Delta 8/\Delta 8}$ homozygous fish to generate G2 $TERT^{\Delta 8/\Delta 8}$ embryos (Figure 4A). While G1 $TERT^{\Delta 8/\Delta 8}$ embryos were similar to wild-type embryos (see Figure 3B), G2 $TERT^{\Delta 8/\Delta 8}$ embryos showed gross developmental abnormalities (Figure 4B, right panel), and all died prior to hatching (Figure 4C). Thus, the severity of phenotype between generations increases. To test if telomere length is indeed shorter in G2 $TERT^{\Delta 8/\Delta 8}$ embryos compared to wild-type or G1 $TERT^{\Delta 8/\Delta 8}$ embryos, we used Terminal Restriction Fragment (TRF) Southern blot on genomic DNA isolated from $TERT^{+/+}$, G1 $TERT^{\Delta 8/\Delta 8}$, or G2 $TERT^{\Delta 8/\Delta 8}$ individual live embryos, using a radio-labeled telomeric probe. These Southern blots revealed that the average length of telomeres was shorter in G2 $TERT^{\Delta 8/\Delta 8}$ embryos than in wild-type embryos (~1.5 kb versus ~6 kb, respectively) (Figure 4D, left panel) and G1 $TERT^{\Delta 8/\Delta 8}$ embryos (Figures 4D, right panel, and S3). The dramatic telomere shortening in the G2 generation of TERT-deficient fish, coupled with the increase in severity of phenotype, is consistent with genetic anticipation and germline defects. Thus, we have successfully generated a vertebrate model for telomerase deficiency that rapidly recapitulates several characteristics of the corresponding human disease. Our results also provide a proof of principle for the use of genome editing in a naturally short-lived vertebrate as a powerful way to quickly test the function of a gene involved in human disease and aging.

Site-specific precise editing: generating a disease-causing nucleotide mutation in *TERT* and inserting a short sequence in *POLG*

A large proportion of human diseases are not caused by deletions but by single nucleotide mutations that result in amino acid changes (non-synonymous mutations) (Genomes Project et al., 2012). Therefore, we tested the feasibility of editing a specific amino acid residue, taking advantage of homology-directed repair (HDR) instead of the less precise NHEJ (Figure 5A). To this end, we co-injected Cas9 mRNA, one gRNA, and a single-strand DNA (ssDNA) template with a mutation at the desired site to modify the corresponding genomic residue via HDR (Figure 5A) (Bedell et al., 2012). In human TERT, almost all the disease-associated mutations are non-synonymous (Podlevsky et al., 2008), and many are conserved in the turquoise killifish (Figure 5B). We selected an evolutionary conserved lysine (K902 in human TERT) whose mutation to arginine (Parry et al., 2011) or asparagine (Armanios et al., 2005) gives rise to dyskeratosis congenita. This lysine residue corresponds to K836 in the turquoise killifish (Figure 5B). To specifically edit K836, we designed a single gRNA in

the proximity of the region encoding this amino acid and an ssDNA template containing two point mutations: one that changes K836 to R and another that prevents Cas9 from further targeting the edited site (Hsu et al., 2014) (Figure 5C, upper panel). Direct sequencing indeed revealed nucleotide changes leading to the K836R mutation in the turquoise killifish *TERT* (Figure 5C, bottom panel).

We next tested the feasibility of precisely knocking-in a short exogenous sequence using HDR (Figure 5A), this time targeting another candidate gene, the mitochondrial DNA Polymerase γ (*POLG*). We designed a gRNA targeting exon 2 of *POLG* and an ssDNA template containing short homology arms and an exogenous NdeI restriction sequence (Figure 5D, upper panel). We chose to target exon 2 of *POLG*, as it has a very high targeting efficiency (90%, Figure S4). Direct sequencing or digestion with NdeI revealed in-frame knock-in of the NdeI restriction site into the genomic sequence of turquoise killifish *POLG* (Figure 5D, bottom panel). Thus, precise genome-editing allowed us to generate a specific human disease-causing mutation in the turquoise killifish *TERT* gene and knock-in an exogenous sequence in the *POLG* gene.

A toolbox of turquoise killifish mutants encompassing the hallmark of aging

We next sought to use our platform to target various candidate genes within the hallmarks of aging pathways (Lopez-Otin et al., 2013), including cellular senescence and stem cell exhaustion (*p15INK4B*), mitochondrial dysfunction (*POLG*), deregulated nutrient-sensing (*IGF1R, RAPTOR, RPS6KB1*, and *FOXO3*), epigenetic alterations (*ASH2L*), genomic instability (*SIRT6*), loss of proteostasis (*ATG5*), and intercellular communication (*IL8* and *APOE*) (Figures 6A, S4 and Table S1). We targeted genes whose deficiency is expected to either promote longevity (*IGF1R, RAPTOR, RPS6KB1*) or accelerate signs of aging (*TERT, POLG*) (Lopez-Otin et al., 2013). While some genes have already been shown to regulate lifespan in both invertebrates and vertebrates (*IGF1R, RPS6KB1*) (Kenyon, 2010), others have not yet been tested in vertebrates (*ASH2L, FOXO3*) (Figure 6B). Importantly, some genes do not have obvious orthologs in yeast or invertebrates (*p15INK4B, IL8*, and *APOE*) (Figure 6B). Finally, several genes have been implicated in human diseases, including *APOE* (Alzheimer's disease (Rhinn et al., 2013)), *TERT* (dyskeratosis congenita (Armanios, 2009)), and *p15INK4B* (cancer (Okamoto et al., 1995)).

For each of these 13 genes, we assembled gene models and predicted protein sequences, analyzed mRNA expression patterns in 4 tissues, and profiled H3K4me3 epigenetic landscape to determine transcriptional start sites (Figures 6C and S4). We designed 2–5 gRNA sequences for each gene (Table S1), which was sufficient to identify at least one successful gRNA (Figures 6B, 6C, S4 and Table S1). The efficiency of targeting ranged from 0% to 90% depending on the gRNA (Figures 6, S4 and Table S1). So far, we have generated chimeras (F0, adult) for 11 genes (Figure 6B). We have examined germline transmission for 5 of them (*IGF1RA, IGF1RB, ATG5, ASH2L*, and *RPS6KB1*) and report the targeted alleles (Figures 6C and S4). We also have stable lines for a subset of these alleles (Figures 6B and S4, yellow dots and Table S1).

The platform and toolbox we have developed – genome, genomic datasets, gene models, efficient gRNAs – as well as the mutant fish lines will be made available to the community.

To facilitate future design of gRNAs in the turquoise killifish, we have uploaded the sequenced genome and gene models into CHOPCHOP (Montague et al., 2014), thereby providing easy access for the community. Together, our results highlight the ease and versatility of our platform for generating mutants in the turquoise killifish, which will greatly facilitate high throughput aging studies and disease modeling in vertebrates.

Discussion

The turquoise killifish: a new vertebrate model for systematic studies on aging and longevity

Here we developed a platform in a naturally short-lived vertebrate, the turquoise killifish, for the systematic exploration of aging and age-related diseases. The field of aging will greatly benefit from the study of species beyond conventional model systems (Bolker, 2012). Many exceptionally long-lived vertebrates, such as the naked mole rat (~30 years), the Brandt's bat (~30 years), capuchin monkey (~50 years), rock fish (~150 years), and the bow-headed whale (~200 years) (Tacutu et al., 2013) have already allowed comparative genomics, proteomics, and cellular studies (Austad, 2010; Gorbunova et al., 2014). However, long-lived species are not well-suited for genetic manipulation, longitudinal, or lifespan studies. The turquoise killifish, with its naturally short lifespan, well-characterized aging traits, low costs, and ease of maintenance in the laboratory, is highly suited for rapid experimental aging research in vertebrates. Furthermore, the turquoise killifish is currently the shortest living vertebrate with a sequenced genome, which will be valuable for comparative studies.

Fish provide several advantages as laboratory species. They are amenable to high throughput approaches such as genetic and drug screens (Schartl, 2014). Fish also display a range of unique traits. For example, zebrafish, the primary fish model, is widely used for developmental processes due to its unique characteristics (e.g. fast and stereotypic embryonic development). Other fish have been used for specific traits, including social behaviors (cichlids (Fernald, 2012)) and adaptive evolution (sticklebacks (Jones et al., 2012)). Our genome and genome-editing platform in the turquoise killifish should help transition this fish to a more widely studied model, providing a unique opportunity for high throughput aging and longitudinal studies. It will be important to characterize aging in the mutants we have already generated as well as generating additional ones. Finally, the genome-to-phenotype platform we present here could serve as a paradigm for how to rapidly develop a wide range of species into model organisms.

A proof of concept model for telomerase-related pathologies in the turquoise killifish

By targeting the *TERT* gene in the turquoise killifish, we have developed the fastest system so far for studying telomerase pathologies in vertebrates. Similar to what is observed in dyskeratosis congenita patients, TERT-deficient fish exhibit defects in highly proliferative tissues (male germline, intestine, blood) in the first generation and as early as 2 month of age. This killifish *TERT* model should help untangle the interaction between aging and telomerase pathologies, which is largely unknown despite the fact that telomere attrition rate is a good predictor of accelerated aging in humans (Boonekamp et al., 2013). Although TERT-deficient killifish exhibit specific age-dependent defects, we have not observed

premature death by 4–5 months of age. This might indicate that the defects in regeneration of specific tissues are not limiting for lifespan under these conditions, although they may be detrimental under more stressful conditions (e.g. injuries or end of life). It will be important to characterize lifespan, regeneration, and telomere length in this *TERT* model during aging. It will also be interesting to compare the phenotypes of this *TERT* deletion model with models mimicking in killifish the *TERT* mutations found in human patients.

The killifish model fills a unique niche in the wide range of existing models of telomerase deficiency. Cellular models have been extremely helpful to understand telomerase biology and pathologies (Batista and Artandi, 2013), but they cannot easily recapitulate systemic defects or tissue interactions. Invertebrate models, which have provided crucial insights into telomerase function (Raices et al., 2005), lack some of the organs affected by telomere pathologies in humans (e.g. *bona fide* blood) (Gomes et al., 2010). The main vertebrate model system, the laboratory mouse, has been the most widely used to understand the role of telomerase in specific pathologies, particularly cancer (Artandi and DePinho, 2010). However, in laboratory mouse strains, phenotypes are only manifested after several generations because of their extremely long telomeres. This issue can be solved by using the *castaneus* strain, which has shorter telomeres (Hao et al., 2005), but changing genetic background is time-consuming. Recent studies in zebrafish have been promising, with TERT-deficient zebrafish demonstrating a range of phenotypes, including gastrointestinal atrophy, premature infertility, and death (Anchelin et al., 2013; Henriques et al., 2013), although it took those fish at least 6–8 months to exhibit most phenotypes. While the turquoise killifish *TERT* model is still limited by the number of available tools, it should be well suited for rapid exploration of telomere pathologies and screening for potential treatments that can delay these pathologies.

A toolkit for modeling complex human diseases, traits, and drug responses

The advent of personalized medicine and high throughput human genetic studies is providing an overwhelming influx of new variants associated with specific human diseases, traits, and responses to drugs (pharmacogenetics). However, functional validation for most of these genes and variants is lagging behind. One way to study these candidates has been to generate induced pluripotent stem cells (iPSCs) harboring mutations derived from patients or engineered *de novo* (Hockemeyer et al., 2011). Although this approach allows high throughput studies, it does not recapitulate the complex interactions between tissues, such as endocrine and paracrine communication, as well as complex responses to environment or drugs. The turquoise killifish model could greatly facilitate *in vivo* high throughput studies of new candidate genes or alleles, while modeling the integrative and non-cell-autonomous interactions that are characteristic of aging and pathological conditions.

Recent genomic studies have revealed that many human diseases are caused by deleterious non-synonymous variants (Genomes Project et al., 2012), and this is also likely the case for aging and longevity. For example, most disease-causing mutations in human *TERT* are due to variants leading to a single amino acid residue change (Podlevsky et al., 2008). Here we show the feasibility of editing specific sequences in turquoise killifish genes. Such directed knock-in approach will also be particularly helpful for the systematic exploration of variants

in human longevity candidate genes, such as *IGF1R*, which is among ~200 predicted candidates identified by genetic association studies of longevity (Tacutu et al., 2013). This approach could also facilitate introduction of epitope tags, *loxP* sites, or artificial stop codons at endogenous genomic loci.

Overall, our study provides a rapid pipeline for genotype-to-phenotype analyses in a new vertebrate model with a compressed time scale of aging. It also renders available as a resource the *de novo* sequenced genome of the turquoise killifish and mutant lines of this fish. This comprehensive platform opens the possibility of screening for genetic and drug interactions in an integrative system. It also offers a promising venue for high throughput modeling of aging and complex human diseases *in vivo.*

Experimental Procedures

Additional details are provided in the Extended Experimental Procedures.

Gene model prediction, conservation, and phylogeny

Gene models were obtained from 2 independent sources: i) a *de novo* whole-genome shotgun assembly (Genbank JNBZ00000000) ii) a *de novo* transcriptome assembly from 4 adult fish tissues (brain, liver, testis, tail) using Oases (Schulz et al., 2012) (Sequence Read Archive [SRA] SRP041421). For the *de novo* transcriptome assembly, putative annotations were obtained by unidirectional blastx to the Swissprot database. The detailed genome assembly and annotation will be reported elsewhere (D.R.V., B.A.B., P.P.S., and A.B., unpublished data).

Strand-specific RNA-seq expression analysis

RNA extraction was performed using the Nucleospin kit (Machery-Nagel), followed by rRNA removal (Ribozero Magnetic Gold Kit, Epicentre). Double-strand cDNA was ligated with barcoded adapters and amplified using Illumina PCR primers (P1.0 and 2.0, Illumina) prior to sequencing. Expression data was analyzed by mapping RNA-seq reads onto gene models using Tophat2 v2.0.4 and Cufflinks v2.0.2.

H3K4me3 ChIP-seq

H3K4me3 ChIP-seq experiments were performed according to (Benayoun et al., 2014) on whole brain tissue isolated from adult male fish (SRA SRP045718).

CRISPR/Cas9 target prediction for guide RNA selection

For each selected gene, we identified conserved regions in the coding sequence using multiple vertebrate orthologs using http://genome.ucsc.edu/. Conserved regions that were upstream of functional or active protein domains were selected for targeting. Guide RNA (gRNA) target sites were identified using ZiFiT (http://zifit.partners.org/) (Hwang et al., 2013) or CHOPCHOP (https://chopchop.rc.fas.harvard.edu/) (Montague et al., 2014).

Guide RNA synthesis

Initial experiments were performed using the DR274 guide RNA expression vector (Addgene #42250) (Hwang et al., 2013). In subsequent experiments, hybridized oligonucleotides were used as an *in vitro* transcription template. gRNAs were *in vitro* transcribed and purified using the MAXIscript T7 kit (Life Technologies).

Production of Cas9 mRNA

Initial experiments were performed using the MLM3613 Cas9 expression vector (Addgene, #42251) (Hwang et al., 2013). In subsequent experiments, the pCS2-nCas9n expression vector was used (Addgene, #47929) (Jao et al., 2013). Capped and polyadenylated Cas9 mRNA was *in vitro* transcribed and purified using either the mMESSAGE mMACHINE T7 ULTRA or SP6 kits (Life Technologies).

Single-stranded DNA template for homology-directed repair

For homology-directed repair (HDR) experiments, single-stranded DNA (ssDNA) templates were designed to contain short homology arms (30bp–50bp) surrounding the gRNA target. The ssDNA templates were commercially synthesized and purified prior to injection (QIAquick Nucleotide Removal Kit, QIAGEN) (Bedell et al., 2012).

Microinjection of turquoise killifish embryos and sequencing of targeted sites

Microinjection of turquoise killifish embryos was performed according to (Valenzano et al., 2011). Cas9-encoding mRNA (200–300ng/μl) and gRNA (30ng/μl) were mixed with phenol-red (2%) and co-injected into one-cell stage fish embryos. For HDR experiments, the ssDNA template (20μM) was also co-injected. Three days after injection, genomic DNA was extracted from 5–10 pooled embryos. The genomic area encompassing the targeted site (~600bp) was PCR-amplified. Endonuclease digestions or DNA sequencing was used for analysis (Table S1).

Fish husbandry, telomerase activity and telomere length measurements, fertility, histology, and blood count analyses are provided in the Extended Experimental Procedures

Supplementary Material

Refer to Web version on PubMed Central for supplementary material.

Acknowledgments

We thank Summer Thyme, John Geisinger, Franklin Zhong and Michael Bassik for stimulating scientific discussion and members of the Brunet lab, especially Lauren Booth and Ashley Webb for critical discussion and feedback on the manuscript. We thank Brock Martin and Andrew Connolly for histology advice. We thank Tessa Montague, Eivind Valen and James Gagnon for incorporating the genome into the CHOPCHOP search engine. This work was supported by NIH DP1AG044848 and the Glenn Laboratories for the Biology of Aging (A.B.), the Damon Runyon, Rothschild and HFSP fellowships (I.H.), and the Dean's fellowship, Stanford (B.A.B.).

References

Alter BP, Giri N, Savage SA, Rosenberg PS. Cancer in dyskeratosis congenita. Blood. 2009; 113:6549–6557. [PubMed: 19282459]

Anchelin M, Alcaraz-Perez F, Martinez CM, Bernabe-Garcia M, Mulero V, Cayuela ML. Premature aging in telomerase-deficient zebrafish. Dis Model Mech. 2013; 6:1101–1112. [PubMed: 23744274]

Armanios M. Syndromes of telomere shortening. Annu Rev Genom Hum Genet. 2009; 10:45–61.

Armanios M, Chen JL, Chang YP, Brodsky RA, Hawkins A, Griffin CA, Eshleman JR, Cohen AR, Chakravarti A, Hamosh A, et al. Haploinsufficiency of telomerase reverse transcriptase leads to anticipation in autosomal dominant dyskeratosis congenita. Proc Natl Acad Sci U S A. 2005; 102:15960–15964. [PubMed: 16247010]

Artandi SE, DePinho RA. Telomeres and telomerase in cancer. Carcinogenesis. 2010; 31:9–18. [PubMed: 19887512]

Austad SN. Cats, “rats,” and bats: the comparative biology of aging in the 21st century. Integr Comp Biol. 2010; 50:783–792. [PubMed: 21558241]

Batista LF, Artandi SE. Understanding telomere diseases through analysis of patient-derived iPS cells. Curr Opin Genet Dev. 2013; 23:526–533. [PubMed: 23993228]

Bedell VM, Wang Y, Campbell JM, Poshusta TL, Starker CG, Krug RG 2nd, Tan W, Penheiter SG, Ma AC, Leung AY, et al. In vivo genome editing using a high-efficiency TALEN system. Nature. 2012; 491:114–118. [PubMed: 23000899]

Benayoun BA, Pollina EA, Ucar D, Mahmoudi S, Karra K, Wong ED, Devarajan K, Daugherty AC, Kundaje AB, Mancini E, et al. H3K4me3 Breadth Is Linked to Cell Identity and Transcriptional Consistency. Cell. 2014; 158:673–688. [PubMed: 25083876]

Bessler M, Wilson DB, Mason PJ. Dyskeratosis congenita. FEBS Lett. 2010; 584:3831–3838. [PubMed: 20493861]

Bolker J. Model organisms: There’s more to life than rats and flies. Nature. 2012; 491:31–33. [PubMed: 23128209]

Boonekamp JJ, Simons MJ, Hemerik L, Verhulst S. Telomere length behaves as biomarker of somatic redundancy rather than biological age. Aging Cell. 2013; 12:330–332. [PubMed: 23346961]

Di Cicco E, Tozzini ET, Rossi G, Cellerino A. The short-lived annual fish *Nothobranchius furzeri* shows a typical teleost aging process reinforced by high incidence of age-dependent neoplasias. Exp Gerontol. 2011; 46:249–256. [PubMed: 21056099]

Fernald RD. Social control of the brain. Annu Rev Neurosci. 2012; 35:133–151. [PubMed: 22524786]

Genade T, Benedetti M, Terzibasi E, Roncaglia P, Valenzano DR, Cattaneo A, Cellerino A. Annual fishes of the genus *Nothobranchius* as a model system for aging research. Aging Cell. 2005; 4:223–233. [PubMed: 16164422]

Abecasis GR, Auton A, Brooks LD, DePristo MA, Durbin RM, Handsaker RE, Kang HM, Marth GT, McVean GA. Genomes Project C. An integrated map of genetic variation from 1,092 human genomes. Nature. 2012; 491:56–65. [PubMed: 23128226]

Gomes NM, Shay JW, Wright WE. Telomere biology in Metazoa. FEBS Lett. 2010; 584:3741–3751. [PubMed: 20655915]

Gorbunova V, Seluanov A, Zhang Z, Gladyshev VN, Vijg J. Comparative genetics of longevity and cancer: insights from long-lived rodents. Nat Rev Genet. 2014; 15:531–540. [PubMed: 24981598]

Hao LY, Armanios M, Strong MA, Karim B, Feldser DM, Huso D, Greider CW. Short telomeres, even in the presence of telomerase, limit tissue renewal capacity. Cell. 2005; 123:1121–1131. [PubMed: 16360040]

Hartmann N, Englert C. A microinjection protocol for the generation of transgenic killifish (Species: *Nothobranchius furzeri*). Dev Dyn. 2012; 241:1133–1141. [PubMed: 22473915]

Hartmann N, Reichwald K, Lechel A, Graf M, Kirschner J, Dorn A, Terzibasi E, Wellner J, Platzer M, Rudolph KL, et al. Telomeres shorten while Tert expression increases during ageing of the short-lived fish *Nothobranchius furzeri*. Mech Ageing Dev. 2009; 130:290–296. [PubMed: 19428446]

Henriques CM, Carneiro MC, Tenente IM, Jacinto A, Ferreira MG. Telomerase is required for zebrafish lifespan. PLoS Genet. 2013; 9:e1003214. [PubMed: 23349637]

Hockemeyer D, Wang H, Kiani S, Lai CS, Gao Q, Cassady JP, Cost GJ, Zhang L, Santiago Y, Miller JC. Genetic engineering of human pluripotent cells using TALE nucleases. Nat Biotechnol. 2011; 29:731–734. [PubMed: 21738127]

Hsu PD, Lander ES, Zhang F. Development and applications of CRISPR-Cas9 for genome engineering. Cell. 2014; 157:1262–1278. [PubMed: 24906146]

Hwang WY, Fu Y, Reyon D, Maeder ML, Tsai SQ, Sander JD, Peterson RT, Yeh JR, Joung JK. Efficient genome editing in zebrafish using a CRISPR-Cas system. Nat Biotechnol. 2013; 31:227–229. [PubMed: 23360964]

Jao LE, Wente SR, Chen W. Efficient multiplex biallelic zebrafish genome editing using a CRISPR nuclease system. Proc Natl Acad Sci U S A. 2013; 110:13904–13909. [PubMed: 23918387]

Jinek M, Chylinski K, Fonfara I, Hauer M, Doudna JA, Charpentier E. A programmable dual-RNA-guided DNA endonuclease in adaptive bacterial immunity. Science. 2012; 337:816–821. [PubMed: 22745249]

Jones FC, Grabherr MG, Chan YF, Russell P, Mauceli E, Johnson J, Swofford R, Pirun M, Zody MC, White S. The genomic basis of adaptive evolution in threespine sticklebacks. Nature. 2012; 484:55–61. [PubMed: 22481358]

Kenyon CJ. The genetics of ageing. Nature. 2010; 464:504–512. [PubMed: 20336132]

Kirschner J, Weber D, Neuschl C, Franke A, Bottger M, Zielke L, Powalsky E, Groth M, Shagin D, Petzold A, et al. Mapping of quantitative trait loci controlling lifespan in the short-lived fish *Nothobranchius furzeri*--a new vertebrate model for age research. Aging Cell. 2012; 11:252–261. [PubMed: 22221414]

Lee HW, Blasco MA, Gottlieb GJ, Horner JW 2nd, Greider CW, DePinho RA. Essential role of mouse telomerase in highly proliferative organs. Nature. 1998; 392:569–574. [PubMed: 9560153]

Lopez-Otin C, Blasco MA, Partridge L, Serrano M, Kroemer G. The hallmarks of aging. Cell. 2013; 153:1194–1217. [PubMed: 23746838]

Montague TG, Cruz JM, Gagnon JA, Church GM, Valen E. CHOPCHOP: a CRISPR/Cas9 and TALEN web tool for genome editing. Nucleic Acids Res. 2014; 42:W401–W407. [PubMed: 24861617]

Niccoli T, Partridge L. Ageing as a risk factor for disease. Curr Biol. 2012; 22:R741–R752. [PubMed: 22975005]

Okamoto A, Hussain SP, Hagiwara K, Spillare EA, Rusin MR, Demetrick DJ, Serrano M, Hannon GJ, Shiseki M, Zariwala M, et al. Mutations in the p16INK4/MTS1/CDKN2, p15INK4B/MTS2, and p18 genes in primary and metastatic lung cancer. Cancer Res. 1995; 55:1448–1451. [PubMed: 7882351]

Parry EM, Alder JK, Qi X, Chen JJ, Armanios M. Syndrome complex of bone marrow failure and pulmonary fibrosis predicts germline defects in telomerase. Blood. 2011; 117:5607–5611. [PubMed: 21436073]

Podlevsky JD, Bley CJ, Omana RV, Qi X, Chen JJ. The telomerase database. Nucleic Acids Res. 2008; 36:D339–343. [PubMed: 18073191]

Raices M, Maruyama H, Dillin A, Karlseder J. Uncoupling of longevity and telomere length in *C. elegans*. PLoS Genet. 2005; 1:e30. [PubMed: 16151516]

Reichwald K, Lauber C, Nanda I, Kirschner J, Hartmann N, Schories S, Gausmann U, Taudien S, Schilhabel MB, Szafranski K, et al. High tandem repeat content in the genome of the short-lived annual fish *Nothobranchius furzeri*: a new vertebrate model for aging research. Genome Biol. 2009; 10:R16. [PubMed: 19210790]

Rhinn H, Fujita R, Qiang L, Cheng R, Lee JH, Abeliovich A. Integrative genomics identifies APOE epsilon4 effectors in Alzheimer's disease. Nature. 2013; 500:45–50. [PubMed: 23883936]

Rinn JL, Chang HY. Genome regulation by long noncoding RNAs. Annu Rev Biochem. 2012; 81:145–166. [PubMed: 22663078]

Savage SA, Alter BP. Dyskeratosis congenita. Hematol Oncol Clin North Am. 2009; 23:215–231. [PubMed: 19327580]

Schartl M. Beyond the zebrafish: diverse fish species for modeling human disease. Dis Model Mech. 2014; 7:181–192. [PubMed: 24271780]

Schulz MH, Zerbino DR, Vingron M, Birney E. Oases: robust de novo RNA-seq assembly across the dynamic range of expression levels. Bioinformatics. 2012; 28:1086–1092. [PubMed: 22368243]

Tacutu R, Craig T, Budovsky A, Wuttke D, Lehmann G, Taranukha D, Costa J, Fraifeld VE, de Magalhaes JP. Human Ageing Genomic Resources: integrated databases and tools for the biology and genetics of ageing. Nucleic Acids Res. 2013; 41:D1027–1033. [PubMed: 23193293]

Terzibasi E, Lefrancois C, Domenici P, Hartmann N, Graf M, Cellerino A. Effects of dietary restriction on mortality and age-related phenotypes in the short-lived fish *Nothobranchius furzeri*. Aging Cell. 2009; 8:88–99. [PubMed: 19302373]

Terzibasi E, Valenzano DR, Benedetti M, Roncaglia P, Cattaneo A, Domenici L, Cellerino A. Large differences in aging phenotype between strains of the short-lived annual fish *Nothobranchius furzeri*. PLoS One. 2008; 3:e3866. [PubMed: 19052641]

Trancikova A, Ramonet D, Moore DJ. Genetic mouse models of neurodegenerative diseases. Prog Mol Biol Transl Sci. 2010; 100:419–482. [PubMed: 21377633]

Valenzano DR, Kirschner J, Kamber RA, Zhang E, Weber D, Cellerino A, Englert C, Platzer M, Reichwald K, Brunet A. Mapping loci associated with tail color and sex determination in the short-lived fish *Nothobranchius furzeri*. Genetics. 2009; 183:1385–1395. [PubMed: 19786620]

Valenzano DR, Sharp S, Brunet A. Transposon-mediated transgenesis in the short-lived African killifish *Nothobranchius furzeri*, a vertebrate model for aging. G3 (Bethesda). 2011; 1:531–538. [PubMed: 22384364]

Valenzano DR, Terzibasi E, Cattaneo A, Domenici L, Cellerino A. Temperature affects longevity and age-related locomotor and cognitive decay in the short-lived fish *Nothobranchius furzeri*. Aging Cell. 2006; 5:275–278. [PubMed: 16842500]

Zucchero T, Ahmed S. Genetics of proliferative aging. Exp Gerontol. 2006; 41:992–1000. [PubMed: 17049783]

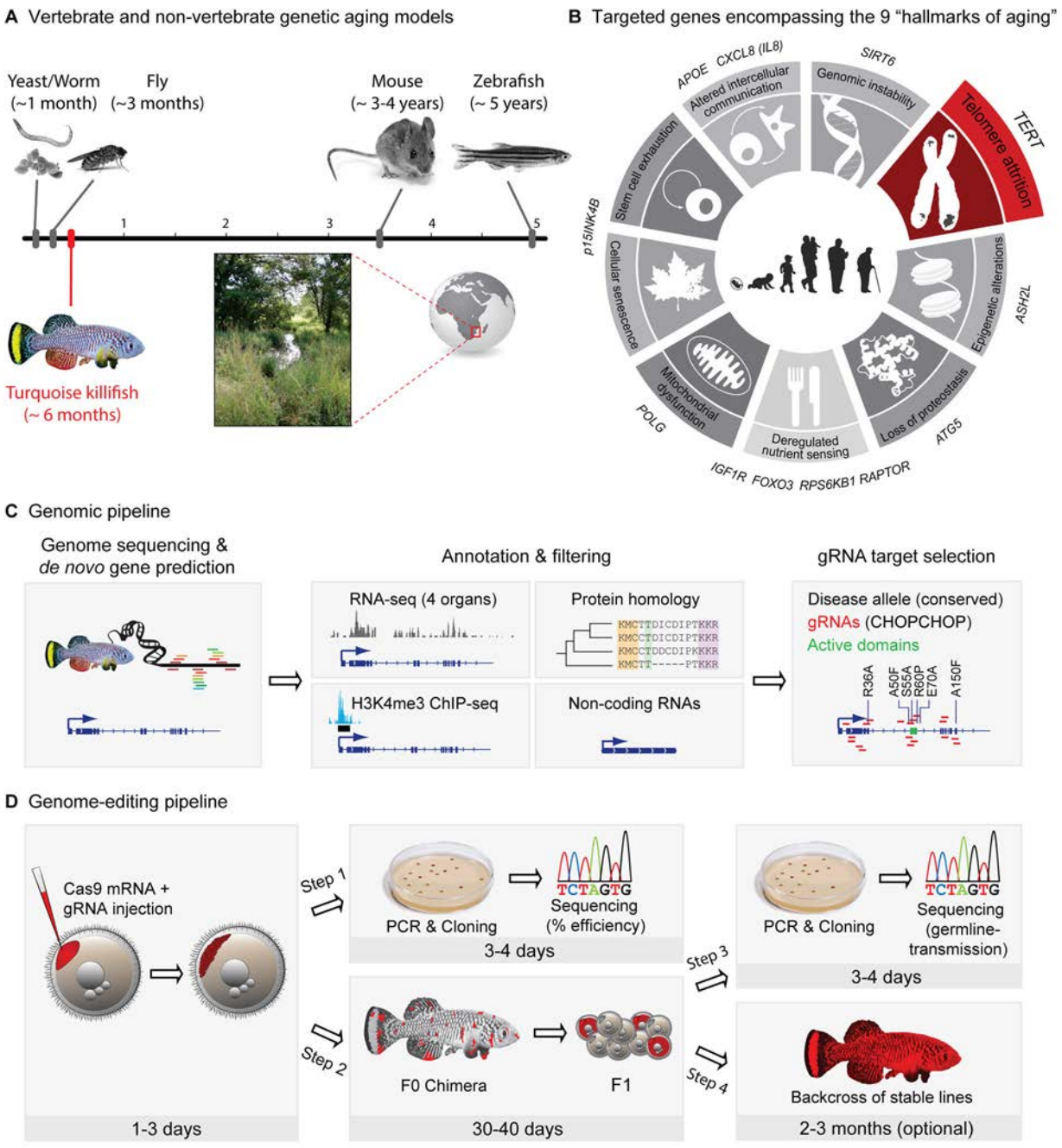

Figure 1. A versatile platform for rapid exploration of aging and longevity genes in the naturally short-lived turquoise killifish

(A) Lifespan of non-vertebrate and vertebrate model systems widely used for aging and disease research (top panel), when compared to the lifespan of the turquoise killifish (bottom panel). The turquoise killifish originates from ephemeral water ponds in Zimbabwe and Mozambique (bottom panel).

(B) Examples of genes encompassing the hallmarks of human aging (modified with permission from (Lopez-Otin et al., 2013)).

(C) Genomic pipeline to generate CRISPR/Cas9 guide RNAs (gRNAs) in a new model organism using our newly created genomic tools (*de novo* assembled turquoise killifish genome, epigenome, and transcriptome). Gene models and gRNA selection are available via CHOPCHOP.

(D) CRISPR/Cas9 genome-editing pipeline to generate stable mutant fish lines in the turquoise killifish. Overall, the total time for generating a stable mutant line in the lab (i.e. steps 1–4) is about 2–3 months.

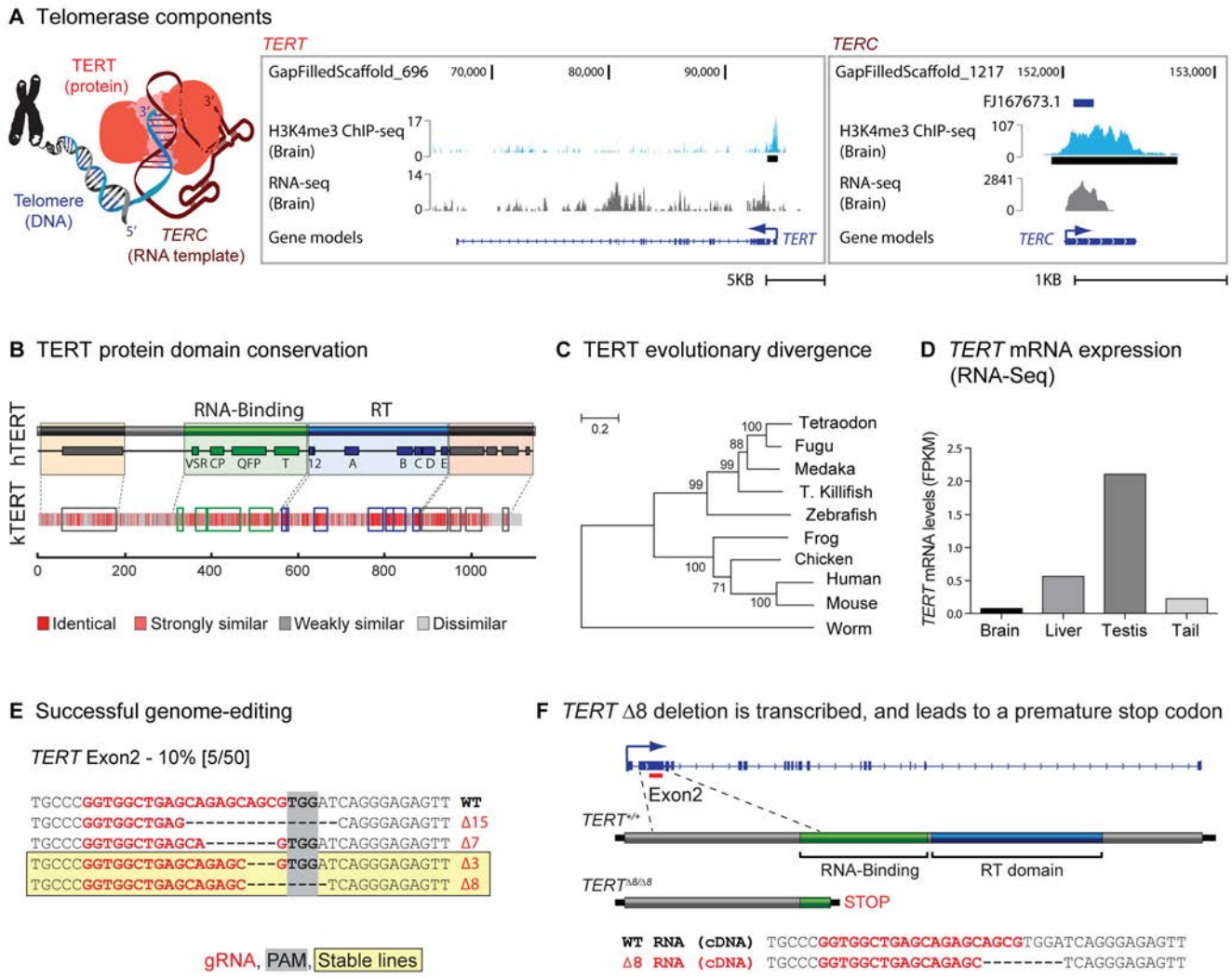

Figure 2. Example of rapid genome-editing of TERT, the protein component of telomerase, in the turquoise killifish

(A) The telomerase complex, and gene model prediction for *TERT* and *TERC* using genomic and epigenomic profiling.

(B) Conservation of TERT protein domains between human (hTERT) and the turquoise killifish (kTERT).

(C) TERT protein sequence divergence predicts evolutionary tree.

(D) Relative expression of *TERT* mRNA in brain, liver, testis and tail using RNA-seq. FPKM: fragments per kilobase of exon per million fragments mapped.

(E) Successful editing of the turquoise killifish *TERT* gene. The wild-type (WT) sequence as well as the length of deletions (Δ) is indicated relative to the protospacer adjacent motif (PAM, in gray) and the guide RNA sequence (gRNA, in red). The deletions that gave rise to stable lines (Δ3 and Δ8) are indicated (in yellow with black outline).

(F) Top panel: location of the gRNA successfully targeting *TERT* exon 2 (red line), which is upstream of the exons encoding TERT catalytic domains. *TERT*Δ8 allele is predicted to generate a protein with a premature stop codon. Bottom panel: the *TERT* Δ8 allele is

successfully transcribed to RNA, as measured by RT-PCR followed by cDNA sequencing. RT: reverse-transcriptase.

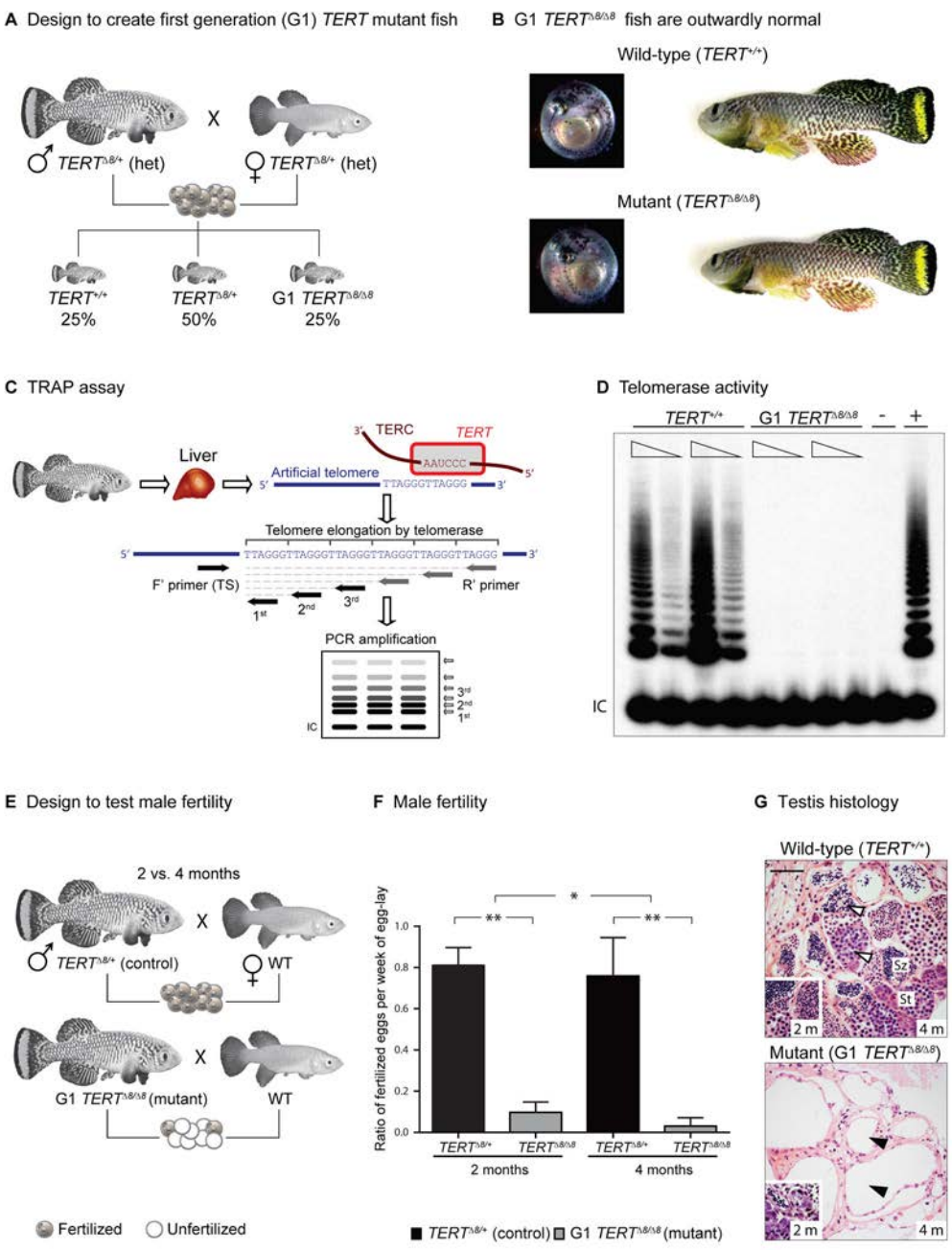

Figure 3. *TERT*$^{\Delta 8/\Delta 8}$ fish show no telomerase activity and exhibit a progressive loss of fertility in the first generation

(A) Intercrossing of *TERT*$^{\Delta 8/+}$ heterozygous (het) fish to generate generation 1 (G1) *TERT*$^{\Delta 8/\Delta 8}$ fish. G1 *TERT*$^{\Delta 8/\Delta 8}$ fish are observed at the expected Mendelian ratios (no difference between expected and observed frequencies, $p = 0.8809$, χ^2 test).

(B) G1 *TERT*$^{\Delta 8/\Delta 8}$ embryos (left panels) and adults (right panels) are outwardly normal.

(C) Schematic for the Telomere Repeat Amplification Protocol (TRAP). Telomerase enzymatic activity in liver is evaluated by the ability of tissue extract to add telomeric repeats to radio-labeled artificial telomeres *in vitro*.

(D) Telomerase enzymatic activity as measured by the TRAP assay in *TERT*$^{+/+}$ and G1 *TERT*$^{\Delta 8/\Delta 8}$ fish liver samples. IC: TRAP internal control product. Representative of 3 independent experiments.

(E) Experimental design to assess male fertility. *TERT*$^{\Delta 8/+}$ (control) and G1 *TERT*$^{\Delta 8/\Delta 8}$ (mutant) males, at two different age groups (2 and 4 months), were mated with young (2 months) wild-type (WT) females. Fertilized eggs (gray) were counted after 1 week.

(F) Ratio of fertilized eggs per week of egg-lay in *TERT*$^{\Delta 8/+}$ (control) and G1 *TERT*$^{\Delta 8/\Delta 8}$ (mutant). Mean±SD of >70 eggs, generated from 4–5 crosses per age group. Wilcoxon signed-rank test, *$p<0.05$, **$p<0.01$. For the comparison between age groups, standardized values to age-matched controls were used.

(G) Histological sections of testis from *TERT*$^{+/+}$ (control) and G1 *TERT*$^{\Delta 8/\Delta 8}$ fish at 4–5 months (4m, full size image) and 2 months (2m, insert). Sz: spermatozoa (mature sperm); St: spermatids. Scale bar: 50μm. Representative of n≥6 individuals from each genotype (4–5 months) and n=2 individuals from each genotype (2 months).

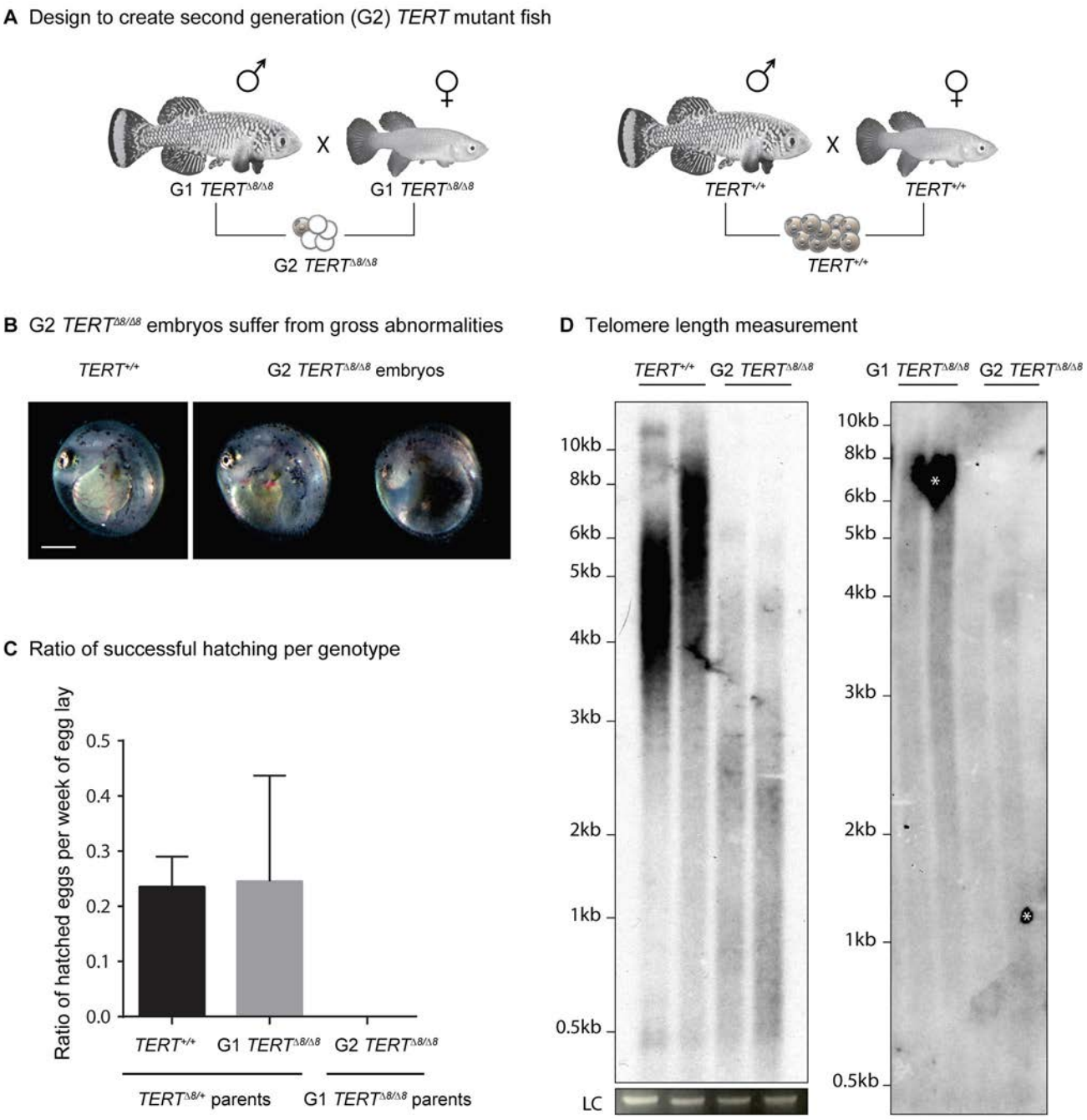

Figure 4. TERT-deficient turquoise killifish exhibit genetic anticipation

(A) Experimental design. G1 $TERT^{\Delta 8/\Delta 8}$ (left) or $TERT^{+/+}$ (right) fish were intercrossed to generate generation 2 (G2) $TERT^{\Delta 8/\Delta 8}$ or $TERT^{+/+}$ fish, respectively. The development of embryos was assessed until hatching.

(B) Representative images of $TERT^{+/+}$ and G2 $TERT^{\Delta 8/\Delta 8}$ embryos at an equivalent developmental stage. Scale bar: 300μm.

(C) Ratio of successful hatching per week of egg-lay for the indicated genotypes. Mean+SD of >70 embryos for each parental genotype ($TERT^{\Delta 8/+}$ versus G1 $TERT^{\Delta 8/\Delta 8}$).

(D) Telomere length measurement using telomere restriction fragment (TRF) Southern-blot. Left panel: $TERT^{+/+}$ and G2 $TERT^{\Delta 8/\Delta 8}$ embryos. Representative of 3 experiments. LC: loading control for genomic DNA. Right panel: G1 $TERT^{\Delta 8/\Delta 8}$ and G2 $TERT^{\Delta 8/\Delta 8}$ embryos. Expanded version is in Figure S3. White asterisk: non-specific probe binding.

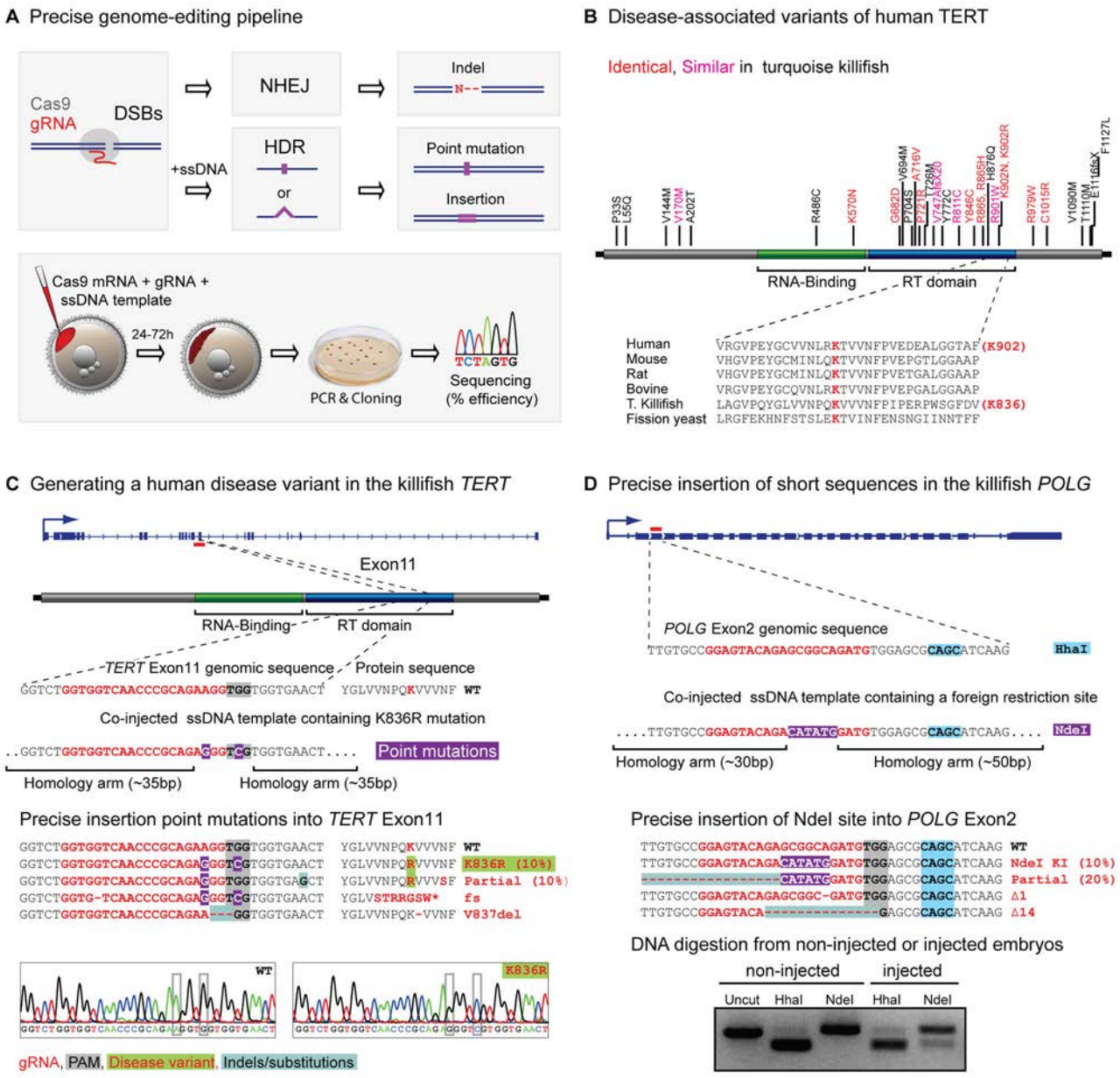

Figure 5. Precise generation of human disease mutation in *TERT* and insertion of a short sequence in *POLG*

(A) Genome-editing pipeline for specific point mutations and insertions. ssDNA: single-strand DNA template. NHEJ: non-homologous end joining. HDR: homology-directed repair.

(B) Top panel: Disease-associated variants in hTERT. Conservation of the disease-causing residues between human TERT and turquoise killifish TERT is color-coded (red: identical, pink: similar in turquoise killifish TERT). Bottom panel: K902 in human TERT is evolutionary conserved and corresponds to K836 in turquoise killifish TERT.

(C) Top panels: Location of a selected gRNA (red line) in close proximity to K836 in exon 11 of the turquoise killifish *TERT*, and core sequence of the co-injected ssDNA template. Bottom panel: precise editing of specific codons leading to the nucleotide change (A to G)

corresponding to the K836R mutation. An example chromatogram is shown at the bottom. The K836R mutation is highlighted with green background. fs: frame shift, del: deletion. (D) Location of the gRNA targeting exon 2 of the turquoise killifish *POLG*, and core sequence of the co-injected ssDNA template to introduce an exogenous NdeI site. Bottom panels: precise insertion of the NdeI restriction sequence, as shown by direct sequencing or restriction digestion. Representative of 2 independent experiments.

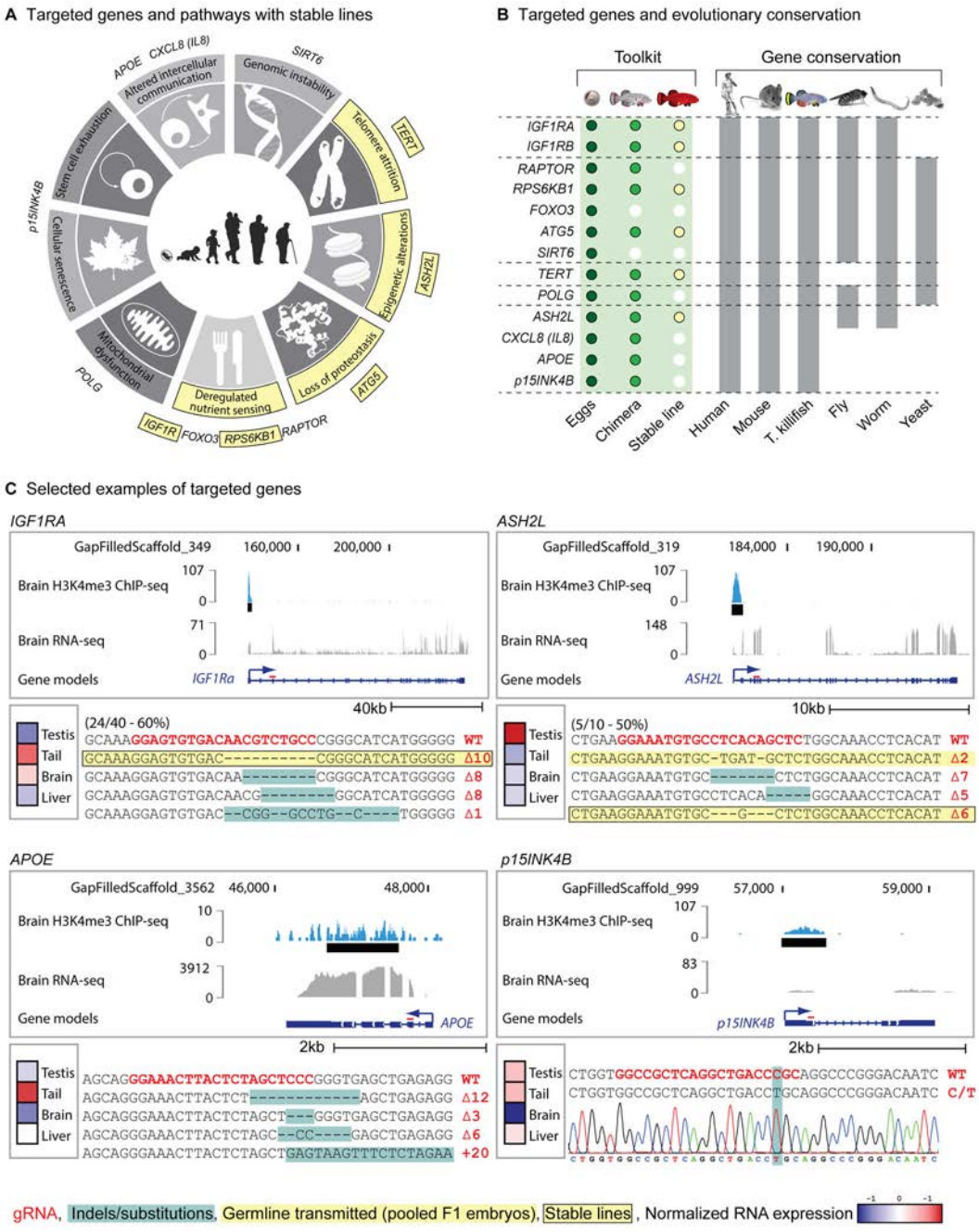

Figure 6. A toolkit for vertebrate aging and age-related disease research

(A) Genes that were successfully edited in the 9 hallmarks of aging. Genes and pathways for which we chose to generate stable lines are indicated in yellow with a black outline.

(B) Detailed stages of editing completion in specific genes, color-coded as indicated. Presence of orthologs in different species is indicated in gray.

(C) Selected examples of targeted genes, depicting detailed genomic, epigenomic and expression information (upper box), relative expression in tissues (lower left box), and types of observed indels and substitutions (lower right box). Germline-transmitted alleles assessed in pooled F1 embryos are in yellow. Stable lines are in yellow with a black outline.

Whenever assessed, the targeting efficiency in eggs was indicated as a percentage. For ASH2L, the Δ6 stable line was generated by a separate pair of founders and was not part of the efficiency calculation. Example of a sequencing chromatogram showing the substitution in *p15INK4B*.